Visual closed-loop dynamics via ocular drift

Liron Gruber and Ehud Ahissar

Department of Neurobiology, Weizmann Institute of Science, Rehovot 76100, Israel

Corresponding Author: ehud.ahissar@weizmann.ac.il

Ehud Ahissar
Professor
Department of Neurobiology
The Weizmann Institute of Science
234 Herzl St.
Rehovot 76100
Israel
http://www.weizmann.ac.il/neurobiology/labs/ahissar/home

Acknowledgements: We thank Amos Arieli for his invaluable help in performing the experiments and Michele Rucci and Rafi Malach for commenting on earlier versions of the manuscript. This research was supported by the European Research Council (ERC) under the European Union's Horizon 2020 research and innovation programme (grant agreement No 786949). E.A. holds the Helen Diller Family Professorial Chair of Neurobiology.

Competing interests: The authors declare no competing financial interests.

Abstract

The human visual system perceives its environment via eye movements, whose primary kinematic components are saccades and drifts. Saccades are quick transitions of the gaze from one Region of Interest (ROI) to another and drifts are slower scanning motions in each ROI. While it is accepted that ROI selection depends on the accumulated visual data, drift is commonly considered not to be affected by the acquired visual information. Here we directly tested the latter assumption by testing the dependency of drift kinematics on the concurrent visual inputs. We tracked ocular kinematics in 5 healthy subjects (3 women) while modulating the available visual information via image size and a gaze-contingent display; the latter was used to tunnel vision to a limited window around gaze center. Our results reveal that visual acquisition and the ocular drift movement are linked via a closed-loop dynamic process. This is demonstrated by (i) a dependency of the drift trajectory on the concurrent visual input (ii) condition-specific convergence of the drift speed (within < 100ms) and (iii) maintenance of selected motor-sensory "controlled variables". As these dynamics cannot be accounted for by an open-loop visual scheme, our results suggest that visual acquisition is inherently a closed-loop process.

Author summary

Our eyes are nothing like a camera. It has long been known that we are actively scanning our visual environment in order to see. Moreover, it is commonly accepted that our fast eye movements, saccades, are controlled by the brain and are affected by the sensory input. However, our slow eye movements, the ocular drifts, are often ignored when visual acquisition is analyzed. Accordingly, visual processing is typically assumed to be based on computations performed on saccade-triggered snapshots of the retinal state. Our work strongly challenges this model and provides significant evidence for an alternative model, a cybernetic one. We show that the dynamics of the ocular drift do not allow, and cannot be explained by, open loop visual acquisition. Instead, our results suggest that visual acquisition is part of a closed-loop process, which dynamically and continuously links the brain to its environment.

Introduction

The visual system usually perceives its environment during egomotion [1-3]. In particular, retinal encoding results from continuous interactions between eye movements and the environment [1, 4-9]. The kinematics of eye movements contain two major motion components: saccades, which quickly (speeds between ~10 to ~1000 deg/s) shift the gaze from one ROI to another [10-12] and drifts, which slowly (speeds < ~10 deg/s) scan each ROI [1, 13-15]. These kinematic components, saccades and drifts, characterize the movements of the eyes during every class of ocular function, whether while fixating, pursuing moving targets, reading or exploring. Saccades are often divided to macro and

micro-saccades, shifting the gaze to targets beyond or within the foveal field, respectively. It is currently accepted that all saccades can be characterized along the same kinematic continuum, controlled by the same circuits, and serve the same function – shifting the gaze to a new, overlapping or non-overlapping ROI [14, 16-19]. Hence, here we analyze all saccades in one category.

Two contrasting perceptual schemes might be consistent with this saccade-drift kinematic pattern: an open-loop computational and a closed-loop dynamical scheme. In both schemes, saccades are controlled, at least in part, in a closed-loop manner in which ROI selection depends on the accumulated visual information [10, 11, 19-23]. The two schemes, however, divide in their assumed acquisition process in between saccades. The computational scheme assumes that at each ROI the visual system acquires one snapshot of the ROI per saccade and computes its internal representation through an open-ended sequence of computations, much like in current computer-vision implementations [24-28]. The dynamical scheme, in contrast, assumes that the acquisition of each ROI is a continuous closed-loop process, whose dynamics are determined by the interactions between the drift motion and the external image [29-33].

As a result, the two schemes entail contrasting predictions. (i) The computational scheme predicts that the ocular drift will not depend on the concurrent visual input, whereas the dynamical scheme predicts that it will. (ii) The dynamical scheme further predicts that the drift will exhibit convergence dynamics during perception, as expected from the dynamics of a closed-loop system around its attractors [33]; the computational scheme predicts that drift dynamics should follow a predetermined or random pattern. (iii) Lastly, with closed-loops, adaptive changes are part of a process in which the values of a set of variables, the

"controlled variables", are actively maintained within a certain range that allows the current functioning of the system [33-35]. Open-loop systems do not have this active capacity and depend on a-priori mapping between environmental and internal variables.

To test the predictions of the two schemes, we measured ocular behavior while modulating the available spatial information by reducing image size and by mimicking tunnel vision. We tracked subjects' gaze while they were viewing simple shapes of two sizes, and while revealing to them either the entire visual field ("natural viewing") or only a portion of the image around the center of their gaze ("tunneled viewing"). Ocular dynamics were not consistent with the open-loop scheme, and consistent with visual acquisition being a continuous closed-loop dynamical process.

Methods:

Subjects. 5 healthy subjects with normal vision at the ages 21-28 participated in the experiments (3 females, 2 with right dominant eye, 3 with left dominant eye). All subjects were given detailed explanation about the eye tracker device and the behavioral task, and were paid for their participation. Informed consents were obtained from all subjects, in accordance with the approved Declaration of Helsinki for this project.

Experimental Setup. The experiment took place in a darkened and quiet room where subjects sat in front of a high-resolution, fast computer screen (VPixx, 1920x1080, 120Hz). The movements of the dominant eye were recorded using EyeLink II at 100Hz (enabling real time screen manipulation) while the other eye was blindfolded. Subjects sat 1 meter away from the screen and placed their chin on a chinrest to reduce head movements.

Stimuli and gaze windows. Two kinds of images were created: 'large' and 'small', and each was associated with a specific gaze window – a horizontal rectangle centered on the subject's gaze at each sample and through which the image was exposed. The large shapes occupied 10.80±0.15x10.80±0.15 deg (720±10x720±10 pixels), and the large gaze window was 2.90±0.15x1.90±0.15 deg (190±10x130±10 pixels). The small shapes occupied 0.90±0.03x0.90±0.03 deg (60±2x60±2 pixels) with a gaze window of 0.24±0.03x0.16±0.03 deg (13±2x9±2 pixels). The ratio between image and window size was the same for both image sizes (**Videos S1, S2**).

Experimental Design. We tested the performance of subjects in a five forced choice shapes recognition tasks. In each trial, one out of five filled gray basic shapes against a black background was presented (square, rectangle, circle, triangle and a parallelogram; see **Fig. 1a**). These images were presented in two forms, large and small, as described above. Subjects were tested during 5 days. During days 1-3 they performed 2 tunneled vision sessions, the first one with large images and the second one with small images. On day 4 they performed two additional tunneled vision sessions with small images. On day 5 they performed 4 sessions of natural viewing, 2 repetitions with each image size: large, small, large, and small (natural trials were only performed after all tunneled trials ended, to avoid familiarity with the shapes). Each tunneled trial lasted up to 30 s, mean trial duration for tunneled large was 9+2 s and for tunneled small 20+4 s (trials with natural viewing lasted 3 s, hence all comparative analyses were further verified using only the first 3 s of all tunneled trials, to control for trial length confounds, **Table S1**). There were at least 2 repetitions of each shape in each session (10-12 trials per session, only the first two repetitions of each shape were used for analysis), and hence each session lasted up to 12

minutes. Before the beginning of each trial the eye tracker was recalibrated [36]. We used an adaptive calibration method: subjects fixated on a '+' and waited until the gaze report of the eye tracker (marked as 'X') stabilized. The error between the two markers was used to correct the eye tracker's output during the next trial. At the end of each trial subjects reported which of the five shapes was presented, and received a 'correct/wrong' feedback. In the tunneled vision sessions, subjects had to identify a shape that was "hidden" on the screen and exposed only through the gaze window (see above). In the natural vision sessions, subjects had to identify the same shapes, naturally viewing them with no constrains.

Eye movement processing. A velocity based algorithm [modified from Bonneh et al. [37]] was used for detecting all saccades and drift. We used the following threshold parameters for saccades detection: 16 deg/s minimal peak velocity and 0.3 deg minimal amplitude. Each detected saccade was visually examined to verify the quality of saccadic detection. Fixation periods between saccades were labeled drift only if they lasted > 30 ms. Upper bounds of the instantaneous drift speed were computed as the derivative of the raw eye position signal (100Hz). Lower bounds were computed as derivatives of the filtered signals (a third order Savitzky-Golay filter with window size of 3 samples [38]). For **Fig. S2** we in addition used saccadic detection threshold parameters of 3 deg/s for minimal peak velocity and 0.05 deg for minimal amplitude, in order to match and compare previous publications [38].

Borders analysis. Border-following movements during tunneled viewing were those movements in which the border of the shape was visible to the subject during the movement. This was determined by the window size: saccades or drift pauses that started

and ended at less than 1.8 deg (for large), or 0.15 deg (for small) from a border, were classified as “border saccade” or “border drift”, respectively. During natural viewing border-following movements were defined using the same distance criteria.

Curvature index. We defined an index for drift curvature, where *Xp* equals the length of the drift trajectory and *Dp* equals the linear distance between its starting and ending points. Hence, c=0 represents a straight line and c=1 represents a closed curve.

Statistical analyses. Two-tailed t-tests were used to evaluate the significance of differences in the mean values of kinematic variables (*Rs*, *Sp*, *Xp*, *c*), all of which exhibited normal distribution for all subjects. N’s for *Rs* statistics in tunneled-large, natural-large, tunneled-small, natural-small, respectively, were: Subj1 (30,19,30,20); Subj2 (29,20,30,19); Subj3 (27,20,28,18); Subj4 (30,20,30,19); Subj5 (25,20,30,20); N’s for *Sp* and *Xp* statistics were (respectively): Subj1 (1756,229,2392,154); Subj2 (534,110,2626,45); Subj3 (723,129,2108,101); Subj4 (409,104,1288,46); Subj5 (1085,203,2775,136).; Distributions of values were also compared using two-sample Kolmogorov-Smirnov tests. Variances were compared via the corresponding coefficients of variation (CV = variance/mean), using two-sample F-tests. Data are expressed as mean ± S.E.M. Shape presentation order was randomized using a uniform distribution. No blinding was done during analysis and none of the data points was excluded.

Data availability Statement. All analyses were done using MATLAB. All data is available upon request.

Results

Five subjects were asked to identify an image on a screen as one of five options (square, rectangle, circle, triangle and a parallelogram) after viewing it either naturally or through tunneled viewing, during which spatial information was exposed only around the center of their continuously-tracked gaze. Two image sizes and two tunneling windows were used (see **Methods**). Success rates were 100% for natural viewing, 94±6% for the tunneled-large shapes and 60±2% for the tunneled-small shapes. Only correct trials were used for the analysis reported here.

As predicted by the closed-loop nature of ROI selection, which is consistent with both perceptual schemes, limiting the available spatial information had a dramatic effect on gaze locations. During natural viewing of large shapes, the gaze was typically directed around the center of the shape, while during tunneled viewing of large shapes the gaze was typically directed to the borders of the shapes (see examples in **Fig. 1a**). In fact, most (55±7%) of the saccades made by all subjects in all tunneled-large trials were border-saccades, i.e., started and ended near the border (**Fig. 1b**, see **Methods**).

That saccade targets are selected based on previously acquired information had been repeatedly shown. Here, our tunneling results show that target selection can be based on foveal-only information, and on a single fixational pause. With tunneled viewing, saccades were directed along the image borders in a controlled manner (**Fig. 1c** and **Fig. S1),** without being able to acquire any information from the target location prior to landing (mean saccadic amplitude was significantly larger than window size, 3.45±0.07 vs 2.90 deg; $p<0.05$, n= 4648, one-tailed t-test; the large tunneling window is overlaid on the rectangle

example in **Fig. 1a**). Saccadic border-following was evident already at the beginning of each trial and, on average, kept a constant profile along the trial (**Fig. 1d**), suggesting that saccade planning was indeed primarily based on the information collected during the immediately preceding fixational pause(s) rather than on an accumulated estimation of the object's shape.

To better understand how this information is collected in each pause, we examined the dependency of ocular kinematics on concurrent visual acquisition within each fixational pause. We first analyzed the scanning patterns of drifts in ROIs that contained borders. In these ROIs, drift trajectories scanned the image differently if vision was challenged. When challenged by tunneling or a small image size, the eye tended to drift in a curvier pattern when scanning a border, remaining closer to their starting location. The distributions of curvature indexes (see **Methods**) differed between border and non-border drifts in both tunneled conditions ($p<0.05$, Kolmogorov–Smirnov test), and the mean curvature index differed in all conditions ($p<0.05$, two-tailed t-test) except for the natural-large condition ($p=0.7$) (**Fig. 2a**).

The presence of an image border in the field of view had an immediate effect on additional kinematic variable - the speed of the ocular drift (see Methods). The drift speed was significantly lower for border-containing ROIs (**Fig. 2b,** $p<0.05$ in 3 out of the 4 conditions, two tailed t-tests; upper bounds of the drift speed are shown in all figures – see Methods and Discussion). The viewing condition, whether natural or tunneled, had an even stronger effect on drift speed. During tunneled viewing the drift speed was significantly higher than during natural viewing ($p<0.05$, for both image sizes, two tailed t-tests; **Fig. 2b** 1st and 3rd panels versus 2nd and 4th; see also **Fig. S4**).

In addition to a dependency on real-time sensory information, the closed-loop scheme also predicts convergence dynamics [33, 39-41]. Indeed, in all our conditions the ocular drift speed exhibited a converging-like behavior; on average, the drift speed was strongly modulated at the beginning of each pause and gradually converged to an asymptotic value during the pause (**Fig. 2b** and **Fig. S4**). The convergence to an asymptotic target speed value was evident also for individual subjects, and these target speeds were typically stable for the entire durations of the fixational pauses (**Fig. S4**). Importantly, the drift speeds we measured did not depend on the pupil size or on the amplitudes or speeds of the saccades preceding them ($r^2 < 0.01$ for all cases), and these variables were not significantly different across viewing conditions (**Fig. S3**).

The dependency of ocular kinematics on the concurrent sensory information described so far indicate a closed-loop sensory-motor behavior of the visual system and suggest that the closed-loop processing is done at multiple levels, at least those levels controlling saccades and drifts. What may the visual system try to maintain using these loops, and specifically during natural and tunneled perceptual epochs? To address these questions, we analyzed the averaged kinematics in each condition per subject. For most subjects, both saccade average rate (*Rs*, **Fig. 3a**) and mean target drift speed per pause (*Sp*, **Fig. 3b***)* increased in tunneled conditions compared to natural viewing. These differences did not result from the differences in trial length (**Table S1).** Interestingly, the distance travelled during a pause, the "drift length" (*Xp*), did not change for most subjects (**Fig. 3c).**

Assuming that visual information is indeed acquired during fixational pauses [20, 42-45] and that photoreceptors are activated by illumination changes, the mean rate of visual acquisition (during a pause) should be proportional to *Sp* [9, 13] and the amount of visual

information collected during that pause should be proportional to the integrated distance scanned by the eye (the length of its trajectory) during the pause (*Xp*).

Importantly, on average, the tunneling-induced changes in *Rs* and *Sp* compensated each other, keeping *Xp* unchanged, for each stimulus size (**Fig. 4, Table on top**). Thus, when tunneled, the visual system appeared to increase the ROI sampling rate (*Rs*) while maintaining *Xp* and compromising (i.e., loosening) the control of *Sp*. If the control of *Sp* was indeed loosened, the trial-to-trial variability of *Sp* should increase. Indeed, while *Sp* exhibited relatively small coefficients of variation (CVs) during natural viewing (0.90 and 0.57 for large and small, respectively), its CVs increased significantly when tunneled (1.22 and 1.02 for large and small, respectively).

Interestingly, a different strategy appeared with size changes. When viewing small sized images, the visual system decreased the ROI sampling rate while maintaining *Sp* and thus increasing *Xp* (**Fig. 4,** Table insert). A sequential open-loop scheme, in which the visual input affects *Rs and Rs* affects the drift variables, is ruled out here; the mean values of *Rs* did not systematically change along with either *Sp* or *Xp*, and the pause-by-pause correlations between each *Sp* or *Xp* and its preceding instantaneous *Rs* (i.e., the inter-saccadic-interval) were negligible ($R^2 < 0.06$).

Discussion

Consistent with previous reports [13, 46-49], our results demonstrate clearly that ocular drifts are actively controlled by the visual system. What our results add is that this control is part of a closed-loop process - drift kinematics, which affect the visual input, depend on

this very same input. We demonstrate this closed-loop behavior via four major observations. First, we showed that the trajectory of the drift within each ROI depends on the concurrent sensory data. When the drift scanned an ROI that contained an image border its scanning trajectory was controlled to be slower and curvier than when it scanned a non-border ROI (**Fig. 2a,b**). Second, we showed that the drift speed dynamically converges to a condition-specific speed; even when starting with the same speed, the visual system gradually changed its drift speed until it converged to a value that was specific to the viewing condition (**Fig. 2a**). Third, we showed that the system converges to its target speed anew after each saccade within < 100 ms on average (**Fig. 2a**). Such a rapid convergence can only be achieved in loops who's cycle time is significantly smaller than the convergence time – in the visual system these are low-level [certainly sub cortical; [50]] loops. Forth, we found two potential kinematic controlled variables, i.e., drift speed and scanning distance, of the visual acquisition system (**Fig. 4**). Kinematic variables cannot be controlled in an open-loop scheme.

These results do not rule out additional contributions to drift control, other than those of the concurrent visual input, such as experience- and context-dependent biases [13, 47, 48] or slow motor-control processes [52]. Under the closed-loop framework, these broader and slower contributions would operate within higher-level sensory-motor loops [19, 33].

Our measurements are contaminated with measurement noise. With video-based methods, such as the one we used, the major noise sources are inaccurate calibration and changes in the pupil size and head movements [36, 53, 54]. As our results are based on comparisons between conditions measured with the same method, we ruled out the possibility that the differences we found stemmed from differences in pupil size (**Fig. S3**) or insufficient

calibration (we calibrated the device before each trial – see Methods). We could not rule out head movements as a possible additional source of slow kinematics [head movements most likely cannot account for the rapid kinematics demonstrated in **Fig. 2a** [55, 56]]. It is important to note, however, that since head movements always contribute to retinal image-motion [1, 46, 56, 57] their isolation is not required for testing whether visual acquisition is obtained via open- or closed-loop dynamics – head movements are part of these dynamics.

The exact value of the drift speed is not directly accessible to current tracking technologies [8, 58]. We thus assessed the upper and lower bounds of the instantaneous drift speed by analyzing the unfiltered and filtered tracking data, respectively [15]. Along the paper, we use the upper bound speed to compare the ocular dynamics across conditions and demonstrate the basic ocular dynamics during fixational pauses. Thus, the values presented here are higher than those typically presented in the literature, values that are obtained from filtered data (**Fig. S2**). Assuming that the recording noise was similar across the different conditions, comparing ocular kinematics across conditions should yield the same results whether based on the upper or lower bounds. Indeed, this was the case here **(e.g., Fig. S3)**. It should be emphasized here as well, that since all our conclusions are based on comparisons of the same measures across conditions, our conclusions are insensitive to the absolute values of the actual kinematic variables.

Our data suggest that under normal conditions the visual system controls its drift speed such as to maintain it within a specific range [see also [39]]. One plausible reason for such a control is to maintain temporal coding relatively constant at a range suitable for neural processing [8, 19, 59, 60]. When viewing small-size images the visual system does not

compromise this control, possibly for increasing the reliability of sensory data. However, when challenged with tunneled viewing, which decreases the amount of available spatial information, the system compromises the control of drift speed, allowing its increase, for maintaining constant scanning distances under an increased rate of ROI switching (shorter fixational pauses), thus increasing total spatial information. Thus, saccadic ROI switching, which is controlled by both global scene- and task-related factors [5, 10, 11, 14, 18, 61, 62] and local ROI-specific factors [14, 19], appears to be controlled in coordination with the control of the ocular drift (**Fig. 4**). We further show here that this coordination is manifested in real time on a cycle-by-cycle basis (**Fig. 1c,d**).

In our paradigm, the coordinated saccade-drift control maintained, on average, *Sp* across image sizes in natural viewing, and *Xp* across viewing conditions (**Fig. 4**). The identification of these controlled variables was possible only at the population level, and not with individual subjects. This is not surprising, given the complexity of the human visual system and its need to cope with many changing conditions in life. These results, thus, suggest that *Sp* and *Xp* are controlled in most of the individual subjects in the manner described above, as part of a larger set of idiosyncratic controlled variables.

That visual information is acquired continuously along each fixational pause had been demonstrated previously [20, 42-45]. Our results now provide substantial evidence that this acquisition is accomplished by retino-neuro-oculo closed-loops, involving low (certainly subcortical) levels of the visual system. Together with the known closed-loop basis of ROI selection, our results now suggest that vision is inherently a closed-loop process. That is, that all visual processing components are accomplished within brain-environment closed-loops. Being inherently a closed-loop system does not preclude the ability of the visual

system to perceive a certain amount of information even when eye movements are prevented, as often occurs in the laboratory. Being a closed-loop system simply entails, in this context, that every movement of the eye is a component of visual perception and that the system continuously attempts to converge to its attractors [63], getting as close to a given attractor as possible, given the collection of internal and external constrains.

References

1. Steinman RM, Levinson JZ. The role of eye movement in the detection of contrast and spatial detail. In: Kowler E, editor. Eye Movements and Their Role in Visual and Cognitive Processes. Amsterdam: Elsevier; 1990. p. 115-212.
2. Keller GB, Bonhoeffer T, Hubener M. Sensorimotor mismatch signals in primary visual cortex of the behaving mouse. Neuron. 2012;74(5):809-15. Epub 2012/06/12. doi: 10.1016/j.neuron.2012.03.040. PubMed PMID: 22681686.
3. Dadarlat MC, Stryker MP. Locomotion Enhances Neural Encoding of Visual Stimuli in Mouse V1. The Journal of Neuroscience. 2017;37(14):3764-75. doi: 10.1523/jneurosci.2728-16.2017.
4. Barlow HB. Eye movements during fixation. J Physiol. 1952;116:290-306.
5. Yarbus AL. Eye Movements and Vision. New York: Plenum; 1967.
6. Noton D, Stark L. Eye movements and visual perception. Sci Am. 1971;224(6):35-43. PubMed PMID: 5087474.
7. Ditchburn RW. Eye-movements and visual perception. Oxford: Clarendon press; 1973.
8. Rucci M, Ahissar E, Burr D. Temporal coding of visual space. Trends in cognitive sciences. 2018;22(10):883-95.
9. Ahissar E, Arieli A. Figuring space by time. Neuron. 2001;32:185-201. doi: DOI: http://dx.doi.org/10.1016/S0896-6273(01)00466-4.
10. Noton D, Stark L. Scanpaths in eye movements during pattern perception. Science. 1971;171(968):308-11. PubMed PMID: 5538847.
11. Yang SC-H, Lengyel M, Wolpert DM. Active sensing in the categorization of visual patterns. Elife. 2016;5.
12. Meermeier A, Gremmler S, Lappe M. The influence of image content on oculomotor plasticity. Journal of vision. 2016;16(8):17-.
13. Rucci M, Victor JD. The unsteady eye: an information-processing stage, not a bug. Trends in Neurosciences. 2015;38:195-206.
14. Krauzlis RJ, Goffart L, Hafed ZM. Neuronal control of fixation and fixational eye movements. Phil Trans R Soc B. 2017;372(1718):20160205.
15. Ahissar E, Ozana S, Arieli A. 1-D Vision: Encoding of Eye Movements by Simple Receptive Fields. Perception. 2015;44(8-9):986-94.

16. Zuber BL, Stark L, Cook G. Microsaccades and the velocity-amplitude relationship for saccadic eye movements. Science. 1965;150(3702):1459-60.
17. Rolfs M, Kliegl R, Engbert R. Toward a model of microsaccade generation: The case of microsaccadic inhibition. Journal of vision. 2008;8(11):5.
18. Ko HK, Poletti M, Rucci M. Microsaccades precisely relocate gaze in a high visual acuity task. Nature neuroscience. 2010;13(12):1549-53. Epub 2010/11/03. doi: nn.2663 [pii]

10.1038/nn.2663. PubMed PMID: 21037583.
19. Ahissar E, Arieli A, Fried M, Bonneh Y. On the possible roles of microsaccades and drifts in visual perception. Vision research. 2014;118:25-30.
20. Wolf C, Schütz AC. Trans-saccadic integration of peripheral and foveal feature information is close to optimal. Journal of vision. 2015;15(16):1-.
21. Shen K, Paré M. Predictive Saccade Target Selection in Superior Colliculus during Visual Search. The Journal of Neuroscience. 2014;34(16):5640-8.
22. Friston K, Adams R, Perrinet L, Breakspear M. Perceptions as hypotheses: saccades as experiments. Frontiers in Psychology. 2012;3. doi: 10.3389/fpsyg.2012.00151.
23. Wang X, Zhang M, Cohen IS, Goldberg ME. The proprioceptive representation of eye position in monkey primary somatosensory cortex. Nature neuroscience. 2007;10(5):640-6.
24. Crick FHC, Marr DC, Poggio T. An information-processing approach to understanding the visual cortex. In: Schmitt FO, editor. The organization of the cerebral cortex. Cambridge: MIT Press; 1981. p. 505-33.
25. Treisman AM, Gelade G. A feature-integration theory of attention. Cognit Psychol. 1980;12(1):97-136.
26. Pitkow X, Sompolinsky H, Meister M. A neural computation for visual acuity in the presence of eye movements. PLoS Biol. 2007;5(12):e331. Epub 2007/12/29. doi: 07-PLBI-RA-0769 [pii]

10.1371/journal.pbio.0050331. PubMed PMID: 18162043; PubMed Central PMCID: PMC2222970.
27. Poggio T, Serre T. Models of visual cortex. Scholarpedia. 2013;8(4):3516.
28. Cadieu CF, Hong H, Yamins DL, Pinto N, Ardila D, Solomon EA, et al. Deep neural networks rival the representation of primate IT cortex for core visual object recognition. PLoS computational biology. 2014;10(12):e1003963.
29. Uexkull Jv. Theoretical biology. London: K. Paul, Trench, Trubner & co. ltd; 1926.
30. Powers WT. Feedback: beyond behaviorism. Science. 1973;179(71):351-6. PubMed PMID: 4682961.
31. Van Gelder T, Port RF. It's about time: An overview of the dynamical approach to cognition. Mind as motion: Explorations in the dynamics of cognition. 1995;1:43.
32. Kelso JS. Dynamic patterns: The self-organization of brain and behavior: MIT press; 1997.
33. Ahissar E, Assa E. Perception as a closed-loop convergence process. eLife. 2016;5:e12830. doi: http://dx.doi.org/10.7554/eLife.12830.
34. Marken RS. You say you had a revolution: Methodological foundations of closed-loop psychology. Review of General Psychology. 2009;13(2):137.
35. Buckley CL, Toyoizumi T. A theory of how active behavior stabilises neural activity: Neural gain modulation by closed-loop environmental feedback. PLoS computational biology. 2018;14(1):e1005926.
36. Nyström M, Andersson R, Holmqvist K, Van De Weijer J. The influence of calibration method and eye physiology on eyetracking data quality. Behavior research methods. 2013;45(1):272-88.

37. Bonneh YS, Donner TH, Sagi D, Fried M, Cooperman A, Heeger DJ, et al. Motion-induced blindness and microsaccades: cause and effect. Journal of vision. 2010;10(14):22.
38. Cherici C, Kuang X, Poletti M, Rucci M. Precision of sustained fixation in trained and untrained observers. Journal of vision. 2012;12(6):31. Epub 2012/06/26. doi: 10.1167/12.6.31. PubMed PMID: 22728680.
39. Biswas D, Arend LA, Stamper SA, Vágvölgyi BP, Fortune ES, Cowan NJ. Closed-Loop Control of Active Sensing Movements Regulates Sensory Slip. bioRxiv. 2018:366609.
40. Saig A, Gordon G, Assa E, Arieli A, Ahissar E. Motor-sensory confluence in tactile perception. The Journal of Neuroscience. 2012;32(40):14022-32. doi: 10.1523/JNEUROSCI.2432-12.2012. PubMed PMID: 23035109.
41. Horev G, Saig A, Knutsen PM, Pietr M, Yu C, Ahissar E. Motor-sensory convergence in object localization: a comparative study in rats and humans. Philosophical transactions of the Royal Society of London Series B, Biological sciences. 2011;366(1581):3070-6. Epub 2011/10/05. doi: 366/1581/3070 [pii]

10.1098/rstb.2011.0157. PubMed PMID: 21969688; PubMed Central PMCID: PMC3172599.
42. Burr DC. Temporal summation of moving images by the human visual system. ProcRSocLondBBiolSci. 1981;211:321-39.
43. Watt R. Scanning from coarse to fine spatial scales in the human visual system after the onset of a stimulus. JOSA A. 1987;4(10):2006-21.
44. Rucci M, Iovin R, Poletti M, Santini F. Miniature eye movements enhance fine spatial detail. Nature. 2007;447(7146):851-4. Epub 2007/06/15. doi: nature05866 [pii]

10.1038/nature05866. PubMed PMID: 17568745.
45. Grill-Spector K, Kanwisher N. Visual recognition: As soon as you know it is there, you know what it is. Psychological Science. 2005;16(2):152-60.
46. Martinez-Conde S, Macknik SL, Hubel DH. The role of fixational eye movements in visual perception. nature reviews neuroscience. 2004;5(3):229-40. PubMed PMID: 14976522.
47. Rolfs M. Microsaccades: small steps on a long way. Vision research. 2009;49(20):2415-41.
48. Herrmann CJ, Metzler R, Engbert R. A self-avoiding walk with neural delays as a model of fixational eye movements. Scientific Reports. 2017;7(1):12958.
49. Kagan I. Active vision: fixational eye movements help seeing space in time. Current biology : CB. 2012;22(6):R186-8. Epub 2012/03/24. doi: 10.1016/j.cub.2012.02.009. PubMed PMID: 22440800.
50. Schmolesky MT, Wang Y, Hanes DP, Thompson KG, Leutgeb S, Schall JD, et al. Signal timing across the macaque visual system. Journal of neurophysiology. 1998;79(6):3272-8.
51. Sparks DL. The brainstem control of saccadic eye movements. Nature Reviews Neuroscience. 2002;3(12):952.
52. Kowler E, Steinman RM. The effect of expectations on slow oculomotor control. I. Periodic target steps. Vision research. 1979;19(6):619-32.
53. Drewes J, Zhu W, Hu Y, Hu X. Smaller is better: Drift in gaze measurements due to pupil dynamics. PloS one. 2014;9(10):e111197.
54. Ko H-k, Snodderly DM, Poletti M. Eye movements between saccades: Measuring ocular drift and tremor. Vision research. 2016;122:93-104.
55. Skavenski A, Hansen R, Steinman RM, Winterson BJ. Quality of retinal image stabilization during small natural and artificial body rotations in man. Vision research. 1979;19(6):675-83.
56. Poletti M, Aytekin M, Rucci M. Head-eye coordination at a microscopic scale. Current Biology. 2015;25(24):3253-9.

57. Gilchrist ID, Brown V, Findlay JM. Saccades without eye movements. Nature. 1997;390(6656):130-1.
58. Fang Y, Gill C, Poletti M, Rucci M. Monocular microsaccades: Do they really occur? Journal of vision. 2018;18(3):1-14.
59. Ahissar E. Temporal-code to rate-code conversion by neuronal phase-locked loops. Neural Comput. 1998;10(3):597-650.
60. Ahissar E, Arieli A. Seeing via miniature eye movements: A dynamic hypothesis for vision. Frontiers in Computational Neuroscience. 2012;6:89. doi: 10.3389/fncom.2012.00089.
61. Findlay JM, Brown V. Eye scanning of multi-element displays: II. Saccade planning. Vision research. 2006;46(1-2):216-27. PubMed PMID: 16169036.
62. Schütz AC, Braun DI, Gegenfurtner KR. Eye movements and perception: A selective review. Journal of vision. 2011;11(5):9-.
63. Krakauer JW, Ghazanfar AA, Gomez-Marin A, MacIver MA, Poeppel D. Neuroscience needs behavior: correcting a reductionist bias. Neuron. 2017;93(3):480-90.

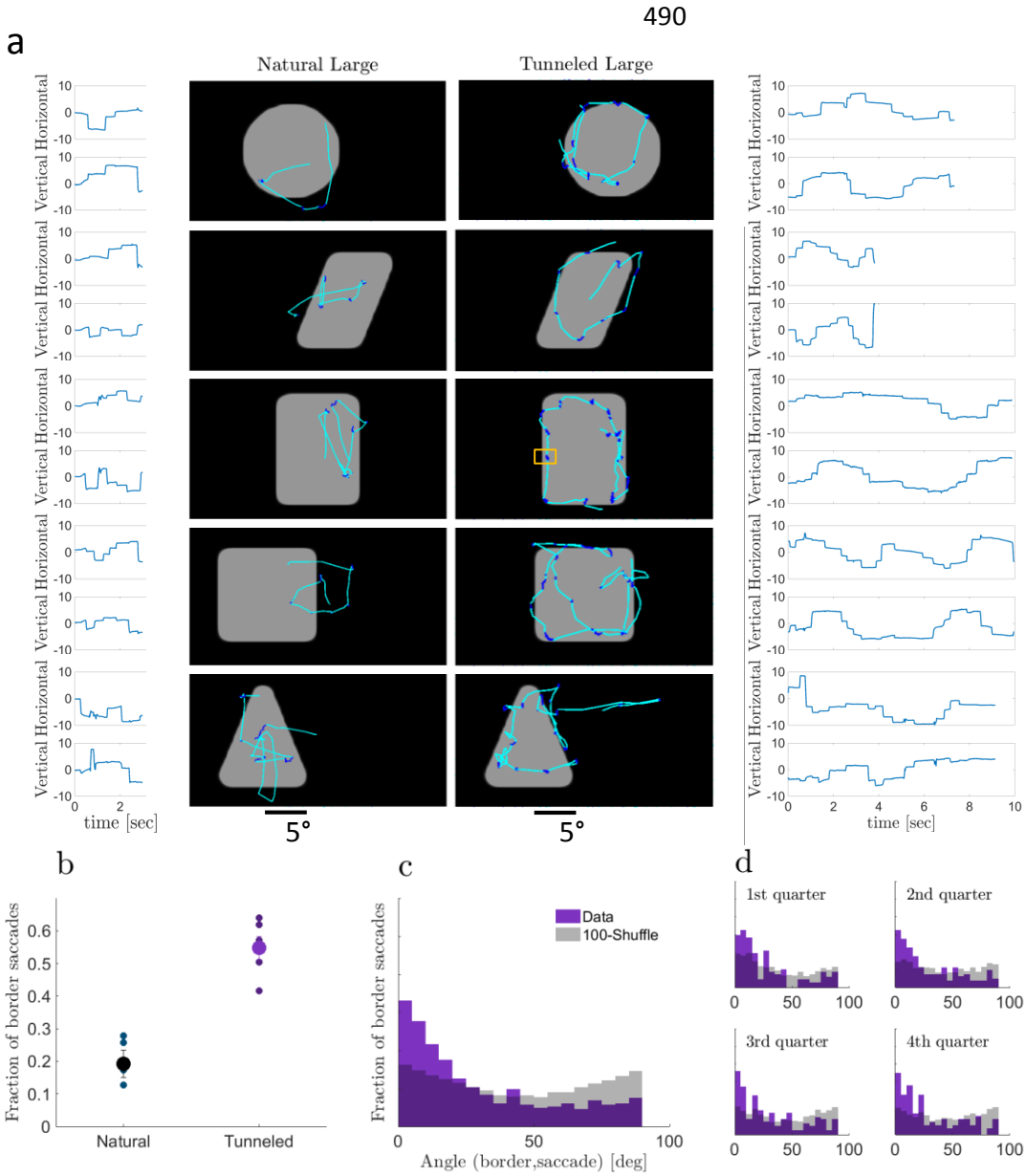
a
Natural Large
Tunneled Large
Vertical Horizontal
time [sec]
5°
5°
b
Fraction of border saccades
Natural
Tunneled
c
Data
100-Shuffle
Fraction of border saccades
Angle (border,saccade) [deg]
d
1st quarter
2nd quarter
3rd quarter
4th quarter

Figure 1. Eye trajectories. (a) Example of eye trajectories in single trials with natural (left) and tunneled (right) large viewing. Saccades, lighter blue; fixational pauses, dark blue; traces, horizontal and vertical components as a function of time next to each example (movies of these examples are in **Videos S3-S7**). **(b)** Fractions of border saccades in the two large conditions for each subject (small dots) and their means (large dots). **(c)** Distribution of the angles between the orientation of the border scanned during a pause and the direction of the immediately following saccade with tunneled large viewing [data shown in purple, shuffled data (saccade directions were shuffled before angle computation; average of 100 repetitions is depicted) in gray; the two histograms are superimposed in the graph, and statistically different, $p<0.05$, two-sample Kolmogorov-Smirnov test]. Analyses of individual subjects are presented in **figure S1-1**. **(d**) Same as (c) for the first, second, third and fourth quarter of each trial. For all, $p<0.05$, two-sample Kolmogorov-Smirnov tests.

514

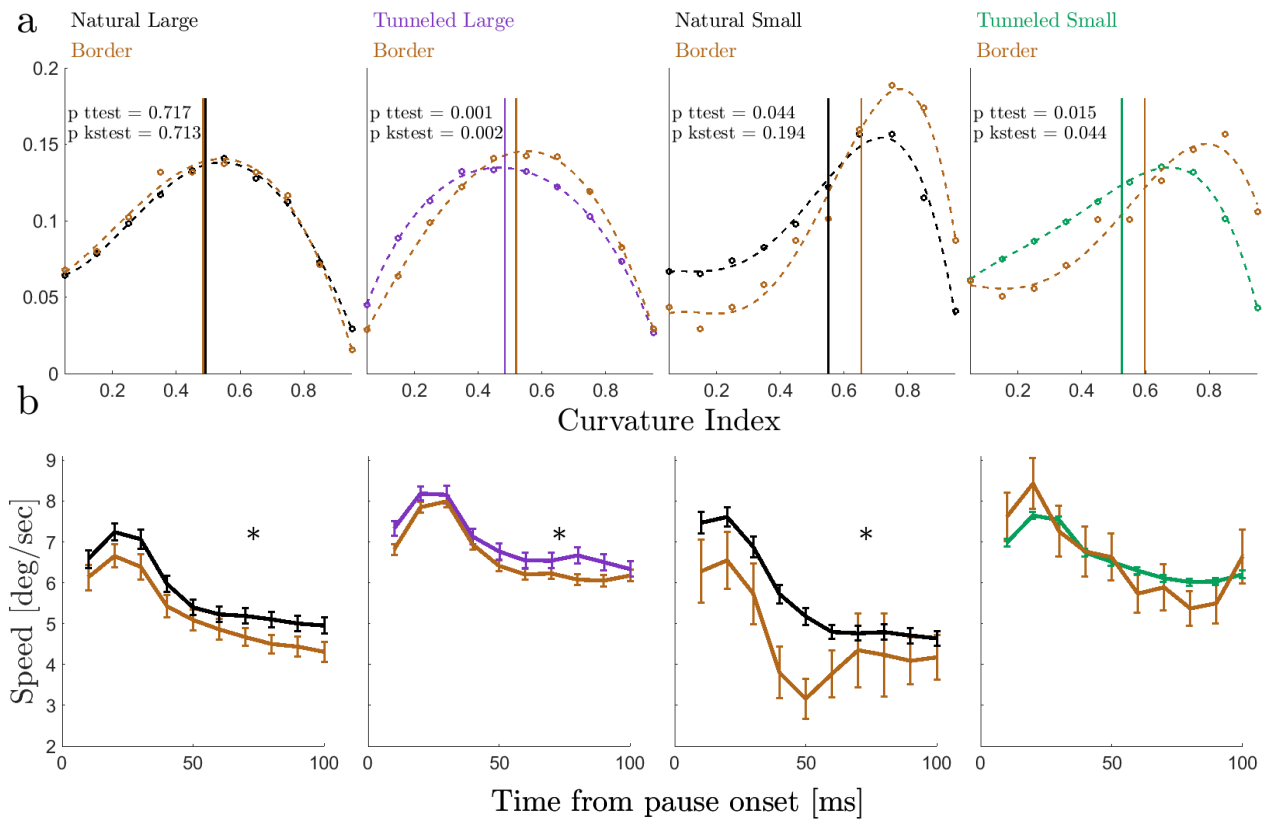
a
Natural Large
Border
Tunneled Large
Border
Natural Small
Border
Tunneled Small
Border
p ttest = 0.717
p kstest = 0.713
p ttest = 0.001
p kstest = 0.002
p ttest = 0.044
p kstest = 0.194
p ttest = 0.015
p kstest = 0.044
Curvature Index
b
Speed [deg/sec]
Time from pause onset [ms]

Figure 2. Drift curvature indices and instantaneous speed. **(a)**. Distributions of curvature indices of border drift trajectories (brown) and non-border drifts trajectories, in the four experimental conditions. Natural viewing in black and tunneled viewing in color (large in purple and small in green). The vertical lines depict the mean values of curvature indices per condition. Mean ± SEM and number of pauses for border and non-border scanning (curvature indices values), respectively: 0.48±0.04 vs. 0.49±0.01 for natural-large (n=192,374 pauses); 0.52±0.01 vs. 0.48±0.01 for tunneled-large (n=1405,757); 0.65±0.05 vs. 0.55±0.02 for natural-small (n=23,270); 0.60±0.03 vs. 0.53±0.01 for tunneled-small (n=66,2723); p-values in each panel are for (i) comparing means using two tailed t-tests and (ii) comparing distributions using two-sample Kolmogorov-Smirnov tests. **(b)** Mean within-pause instantaneous drift speeds of border drift and non-border drifts), in the four experimental conditions (colors as in (a)). Mean ± SEM and number of pauses for border and non-border scanning (target speed values, for time>50ms), respectively: 4.64±0.09 vs. 5.14±0.07 for natural-large (n=143,310 pauses); 6.19±0.05 vs. 6.56±0.07 for tunneled-large (n=863,457); 3.9±0.2 vs. 4.81±0.07 for natural-small (n=19,229); 5.9±0.2 vs. 6.20±0.03 for tunneled-small (n=48,1851); (*, p<0.05, two tailed t-tests).

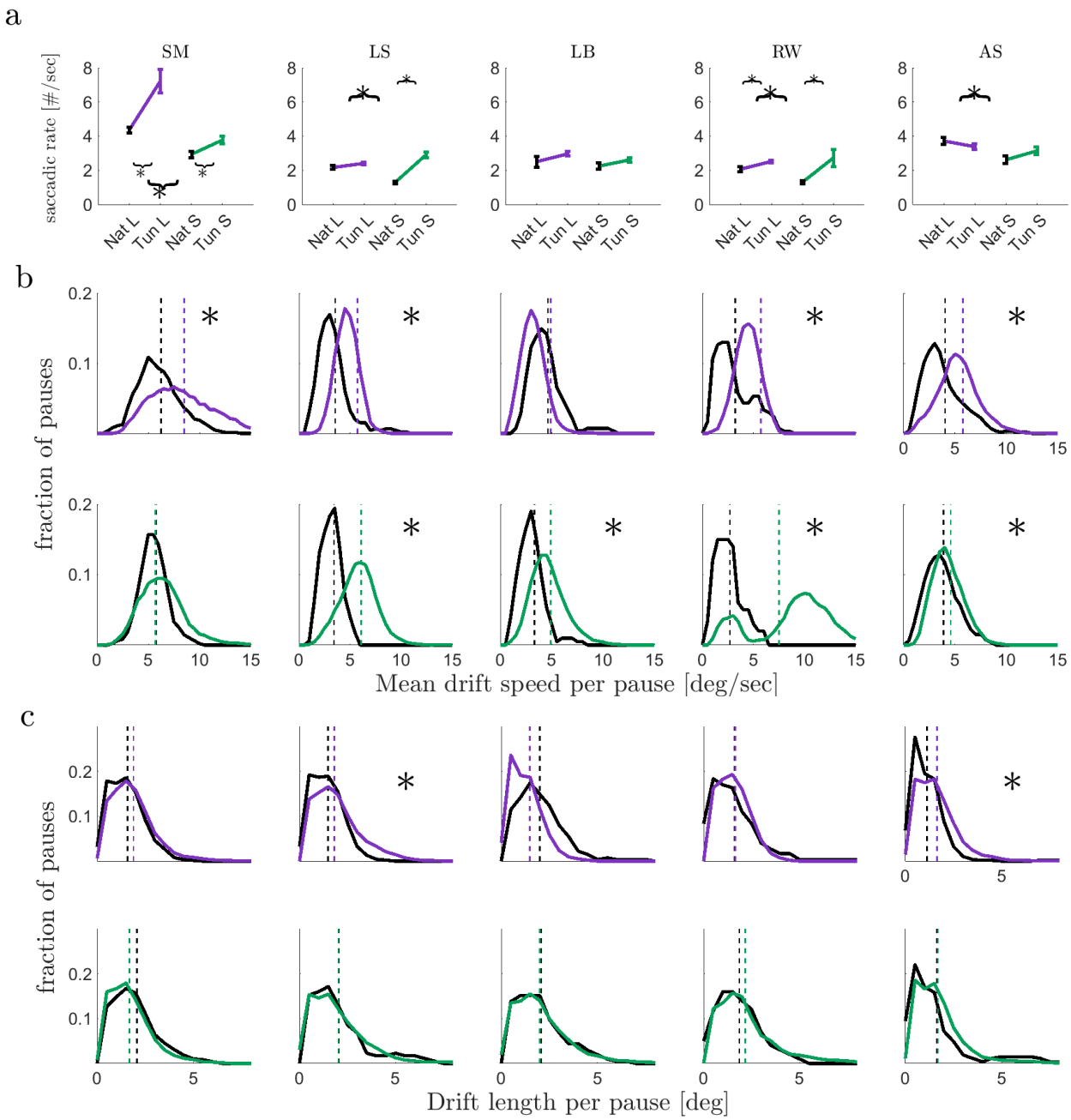
a
SM
LS
LB
RW
AS
saccadic rate [#/sec]
Nat L
Tun L
Nat S
Tun S
b
fraction of pauses
Mean drift speed per pause [deg/sec]
c
fraction of pauses
Drift length per pause [deg]

Figure 3. Kinematics of saccades and drifts. (a) Mean saccadic rates (*Rs*) in natural and tunneled viewing for large (purple) and small (green) image sizes. Data for each subject is presented (*, $p<0.05$, two tailed t-tests). **(b)** Distributions of the mean upper bounds of instantaneous drift speeds (target speed values, for time>50ms) per pause (*Sp*) in the four experimental conditions; data presented as in (a) (*, $p<0.05$, two tailed t-tests). **(c)** Distributions of the distances travelled during a pause (drift length) (*Xp*) in the four experimental conditions; data presented as in (a) (*, $p<0.05$, two tailed t-tests). N's for *Rs* statistics in tunneled-large, natural-large, tunneled-small, natural-small, respectively, were: Subj1 (30,19,30,20); Subj2 (29,20,30,19); Subj3 (27,20,28,18); Subj4 (30,20,30,19); Subj5 (25,20,30,20); N's for *Sp* and *Xp* statistics were (respectively): Subj1 (127,497,97,259); Subj2 (92,164,35,491); Subj3 (55,195,41,415); Subj4 (60,115,20,286); Subj5 (117,347,53,446).

	Sp	*Xp*	*Rs*
NL	4.89±0.09	1.33±0.04	2.9±0.1
TL	5.81±0.05	1.40±0.04	3.7±0.2
NS	4.56±0.09	1.77±0.08	2.0±0.1
TS	5.60±0.03	1.63±0.08	3.0±0.1

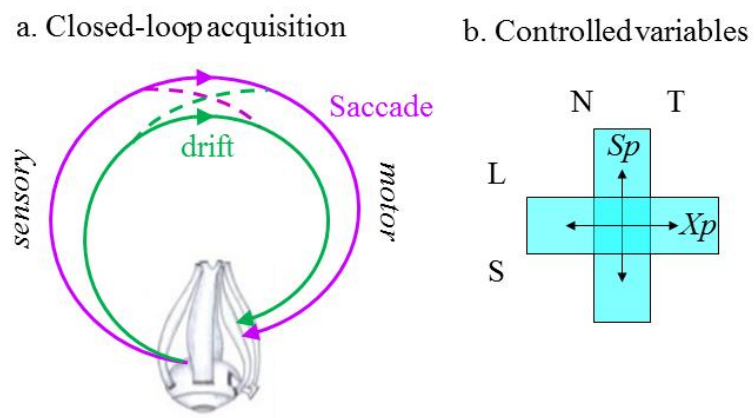

Figure 4. Control variables and closed-loop visual acquisition. (**upper table**) Mean ± SEM of visual scanning variables during each viewing condition (NL, natural large; TL, tunneled large; NS, natural small; TS, tunneled small). *Sp* is the mean instantaneous drift speed during a pause in deg/s, *Xp* is the distance travelled during a pause (drift length) in deg and *Rs* is the mean saccadic rate per trial. Light blue arrows indicate values that do not differ statistically ($p > 0.15$); all other differences were statistically significant ($p < 0.05$). (**a**) Coordinated saccade and drift closed-loops. The two loops interact with each other, coordinating the control of the acquisition. (**b**) Controlled variables. The scheme symbolizes the maintenance of *Sp* across image size (large and small) and the maintenance of *Xp* across viewing conditions (natural and tunneled).